

Electronic Supporting Information

An artificial metalloenzyme that can oxidize water photocatalytically: design, synthesis, and characterization

Ehider A. Polanco^{1,†} and Laura V. Opdam^{1,†}, Leonardo Passerini,² Martina Huber,² Sylvestre Bonnet^{1*} and Anjali Pandit^{1*}

¹*Leiden Institute of Chemistry, Leiden University, Einsteinweg 55, 2333 CC Leiden, The Netherlands*

²*Department of Physics, Huygens-Kamerlingh Onnes Laboratory, Leiden University, Niels Bohrweg 2, 2333 CA, Leiden, The Netherlands*

[†]*Shared first authors with equal contribution to the work*

**corresponding authors: a.pandit@lic.leidenuniv.nl; bonnet@chem.leidenuniv.nl*

Contents

Supplementary A: Materials	2
Supplementary B: Methods and techniques	3
TON, TOF and O ₂ quantum yield determination	7
Protein expression and purification	7
Protein-catalyst complex preparation	8
Water oxidation measurements	9
Supplementary C: Supplementary tables	10
Table S1.	10
Table S2	11
Table S3	11
Table S4.	12
Supplementary D: Supplementary figures	14
Figure S3.	15
Figure S4.	16
Figure S5.	16
Figure S6.	17
Figure S8.	18
Figure S9.	19
Figure S10.	20
Figure S11.	21
Figure S12.	22
Figure S13.	23
Figure S14	24
Figure S15	25
Figure S16	26
Figure S17	27
References	28

Supplementary A: Materials

All chemicals were of analytical grade and were purchased from Sigma Aldrich (Missouri USA) unless stated otherwise. $[\text{Ru}(\text{bpy})_3](\text{ClO}_4)_2$ was synthesized following the reported procedure.¹ Complex N,N'-Bis(salicylidene)ethylenediaminocobalt (II) (catalyst CoSalen) was purchased from Alfa Aesar (Massachusetts, USA). Purified water was obtained using a Milli-Q system (Advantage A10, Merck MilliporeSigma, Jersey USA).

Supplementary B: Methods and techniques

Liquid chromatography-mass spectrometry (LC-MS) was conducted on a Finnigan LCQ Advantage MAX apparatus (Thermo Fisher Scientific, Massachusetts, USA) with a Gemini 3 μm NX-C18 column (Phenomenex, California USA), using a gradient of 10% MeCN in H_2O to 90% MeCN in H_2O with 0.1% TFA as eluent.

High resolution-mass spectrometry (HR-MS) was performed in a Thermo Scientific Q Exactive Orbitrap (ESI+) (Massachusetts, USA) coupled to an Ultimate 3000 nanosystem (3,5 kV; 275 °C; Resolution $R=240.000$ at $m/z=400$; external lock; mass range $m/z=150-1500$) (Thermo Fisher Scientific, Massachusetts, USA). Mobile phase MeCN/ H_2O (1:1 v/v) with 0.1% formic acid, flow= 25 $\mu\text{L}/\text{min}$, direct injection of a 1 μM sample.

Electron spray ionization-mass spectrometry (ESI-MS) was performed with a Synapt G2-Si mass spectrometer from Waters (Massachusetts, USA). Initial separation and denaturing of protein samples was achieved using a nanoEase M/Z protein BEH C4 reversed-phase column, 300 \AA , 1.7 μm x 50 mm, 1/pk (Waters, Massachusetts, USA). Samples were prepared in 10 mM NH_4Ac buffer at pH 7.0 using a Micro Bio-Spin P6 gel desalting column from Bio-Rad (California, USA), maximally 30 min before being run. Deconvolution was performed using the MaxEnt. algorithm of the MassLynx software version 4.2.

UV-vis was measured with an Agilent Cary60 UV-vis spectrophotometer (California, USA) using a quartz cuvette having a 1 cm optical path length. For irradiation experiments followed by UV-vis a 450 nm LED was used as depicted in Figure S1. The power intensity of the LED was set between 19-20 mW using a current of 350 mA, the sample volume was 3 mL, all samples were degassed with Ar for 30 min prior to irradiation and all experiments were performed under constant stirring. A spectrum recorded at $t = 0$ min, *i.e.*, before irradiation, was used as a reference spectrum.

Circular Dichroism (CD) data were recorded with a BioLogic (Tennessee, USA) MOS-500 spectropolarimeter from a 700 μL sample in a 0.2 cm quartz cuvette. A Bio-Logic (Tennessee, USA) SAS lightbox with a Xe lamp as light source was used. An ALX300 power supply was used and always set to 150 W. Data were obtained and processed using Biokine software.

Dynamic light scattering (DLS) measurements were performed with a DynaPro NANOSTAR device from Wyatt technology (Santa Barbara, USA) using a 5 μL cuvette. Data were recorded and processed using the Dynamics 7.10.1.21 software.

Steady-state fluorescence measurements were performed with an F929 Fluorescence spectrometer from Edinburg instruments (Livingston, UK) using a Xe900 lamp as light source and an R928P emission detector. Data were recorded and processed using FS900 software.

For Inductively coupled plasma-mass spectrometry (ICP-MS), the samples were prepared by diluting 20-30 μL of the sample to 200 μL with MilliQ water. Then, concentrated nitric acid (400 μL , 65%) was added to each sample, and the samples were

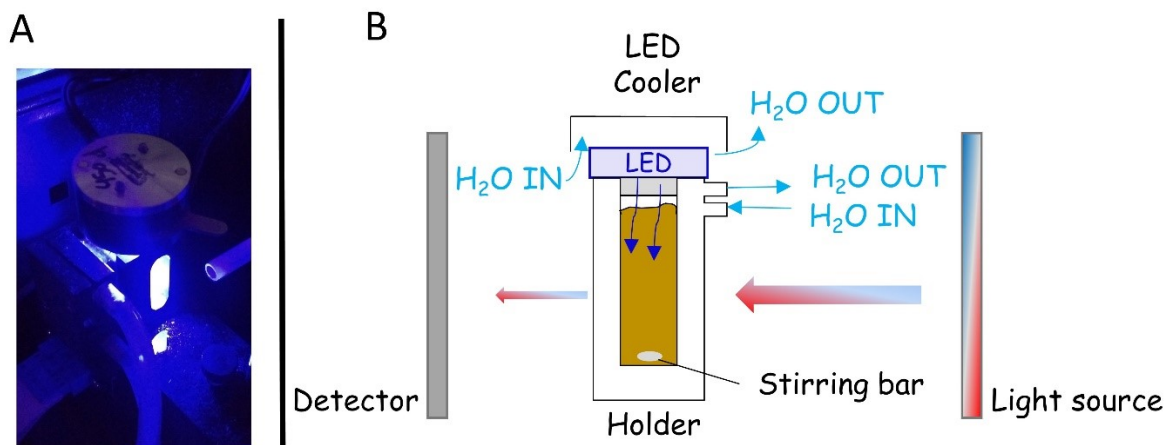


Fig. S1. Irradiation setup for following UV-vis with an integrated cooling system set at 25 °C. Irradiation setup with 450 nm LED on in the UV-vis holder (A). Scheme of the setup of a UV-vis cuvette for irradiation of a sample (B).

digested overnight in the oven in glass test tubes at 90 °C with a glass marble on top. Then 2.4 mL MilliQ water was added to each sample. Afterwards, 1 mL of each sample was diluted with 9 mL of MilliQ water, to reach a total volume of 10 mL (HNO₃ concentration 2.2%). The cobalt and ruthenium concentration of each sample was subsequently measured in triplicate using a NexION 2000 ICP mass spectrometer, an SC2 DX autosampler, and Syngistix software from Perkin Elmer (Massachusetts, USA).

Size exclusion chromatography multi-angle light scattering (SEC-MALS) measurements were performed on a miniDAWN analytical HPLC/FPLC from Wyatt technology (Santa Barbara, USA) using a Superdex 200 Increase 10/300 GL SEC column with eluent 80 mM NaPi + 100 mM NaCl pH 7.5. Data were analysed using the Astra software.

Homology models of *apo*- and *holo*CB5 were generated using Swiss model²⁻⁶. The model of *apo*CB5 is based on the structure of *Rattus norvegicus apo*CB5 from PDB-ID 1IEU⁷ with which it shares 81% sequence identity. The model of truncated *holo*CB5 was based on *Sus scrofa* CB5 from PDB-ID 3X33⁸, with which it shared 97% sequence identity.

Nuclear magnetic resonance (NMR) spectroscopy was measured on a Bruker (Rheinstetten, Germany) AVIII HD 850 MHz (20.0 T) with a TCI cryoprobe. The samples were prepared from protein expressed in ¹⁵N-labelled M9 minimal medium with extra iron so that the total amount is 0.6 g/50 mL in the 10x trace element solution, purified and prepared in the *apo*-state as detailed below and finally buffer exchanged to a 20 mM NaPi buffer at pH 7.5 unless otherwise specified, 6% D₂O was added. All experiments were performed at 293 K, in all spectra the zgpr program for water suppression was used. Large window HSQC spectra were performed with a cnst 4 set to 7 Hz and the receiver gain was kept at 912. Normal HSQC spectra were performed using the hsqcf3gpqh19 pulse program.

For Electron paramagnetic resonance (EPR) analysis, samples containing the solution to analyse were transferred into 4 mm outer diameter EPR quartz tubes and frozen in liquid nitrogen. Continuous wave EPR at X Band (9.5 GHz) was performed on a Bruker Elxsys E680 (Bruker, Rheinstetten, Germany) spectrometer equipped with a TE₁₀₂ cavity and an ESR900 Cryostat (Oxford Instrument, Abingdon, UK). Low temperature was achieved with a constant helium flow. Parameters were the following: modulation amplitude 1 mT, modulation frequency 100 kHz, microwave power 20 mW, total measurement time of 1 h, measurement temperature 10 K. Simulations were performed on MatLab using Easyspin version 5.2.33.⁹

Simulation of the EPR spectrum of CoSalen in buffer was performed with a g tensor of $g = [g_{xx} \ g_{yy} \ g_{zz}] = [5.27 \ 3.85 \ 2.22]$. As line broadening an H-strain was used with the components 3499 MHz, 5235 MHz and 2896 MHz in the respective g tensor

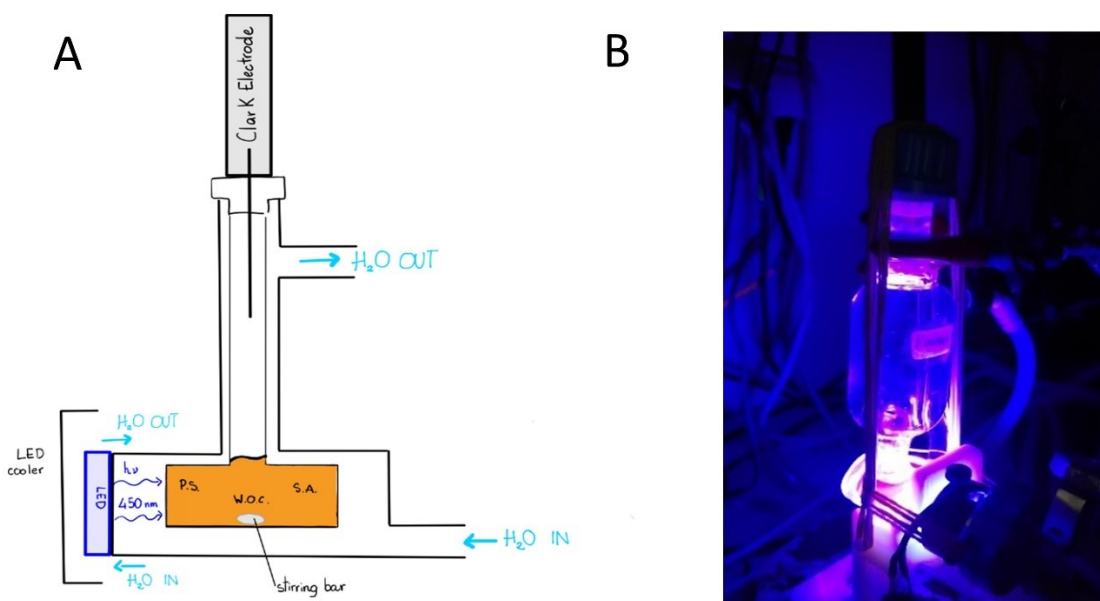


Fig. S2. Water oxidation setup. Integrated cooling system set at 25 °C. Oxygen evolution in the gas phase was detected using a Clark Electrode; the photocatalytic system was closed using hermetic septa on the top to avoid air leakage. Scheme of the irradiation setup for O₂ detection during photocatalytic water oxidation (A). Photograph of the photoreactor setup while irradiating at 450 nm (B).

directions. Simulation of the spectrum of CoSalen in chloroform was performed with an axial g tensor of $g_{xx} = g_{yy} = 2.023$, $g_{zz} = 3.11$ and a hyperfine splitting due to coupling with the $I = 7/2$ ⁵⁹Co nucleus of $A_{zz} = 398$ MHz, which can be seen as eight lines at 230 mT (g_{zz} direction). As line broadening a g -strain was used equal to 0.03 for each one of the g tensor directions.

(Semi-native) Gel electrophoresis was performed using 15% polyacrylamide gels containing 0.1% sodium dodecyl sulphate (SDS). Cracking buffer semi-native PAGE was prepared in absence of SDS and β -mercaptoethanol. The gels were run on a Mini-Protean System and PowerPac Basic Power Supply from Bio-Rad (California, USA) for 50 min at 200 V. The gels were imaged with 2,2,2-trichloroethanol (5 μ L per mL was added to the gel mixture, Sigma Aldrich) or coomassie brilliant blue (gels were fixed prior to staining) as specified with each figure, using a Gel Doc XR+ from Bio-Rad. Gel images were processed using the Image Lab Software version 6.01 from Bio-Rad, adjusting the gamma setting to improve the contrast.

For water oxidation, the setup used was as shown in Figure S2. A 3.5 mL solution in phosphate buffer 80 mM, pH 7.5 containing the adduct CB5:CoSalen, the photosensitizer [Ru(bpy)₃](ClO₄)₂, and the sacrificial electron acceptor Na₂S₂O₈, were placed in a 3.5 mL inner volume photoreactor with an integrated water cooling system settled at 25 °C. Every sample was degassed for 30 min with Ar directly in the reactor and then recorded for 30 min in the dark before irradiation started. 700 rpm stirring speed was set for the reaction. An Unisense (Aarhus, Denmark) Clark electrode needle type sensor (Unisense OX-NP) controlled by x-5 UniAmp with Logger software was used for measuring oxygen concentration in real-time. The sensor was calibrated using pure O₂ as a reference which allowed us to build a calibration curve. The sensor was fixed using a rubber septum and two silicon septa to avoid air leakage as much as possible. O₂ evolution was measured in the gas phase where the tip of the sensor was placed. As a irradiation source, OSRAM opto semiconductors (Regensburg, Germany) 450 nm LED were used. Light power was measured before and after every irradiation to ensure the stability of the light with an OPHIR

(Jerusalem, Israel) Nova-Display laser power meter. Standard ferrioxilate actinometry of each LED was performed to determine the photon flux Φ ($\mu\text{mol s}^{-1}$) using a power source of 350mA: $450e = 9.41\text{E-}08 \mu\text{mol s}^{-1}$ (19 mW); $450f = 1.12\text{E-}07 \mu\text{mol s}^{-1}$ (19 mW); $450g = 1.03\text{E-}07 \mu\text{mol s}^{-1}$ (19 mW).

TON, TOF and O₂ quantum yield determination

The turnover number (TON) was calculated using Equation S1 where η_{O_2} (μmol) is the number of mol of dioxygen produced by the system during an irradiation period of 120 min; η_{CAT} (μmol) is the number of mol of catalyst used in the photocatalytic system.

$$TON = \frac{\eta_{O_2}}{\eta_{CAT}} \quad \text{Equation S1}$$

The O₂ production quantum yield (φ) was calculated according to Equation S2 as reported in the literature:²

$$\varphi = \frac{2\eta_{CAT}TOF_{max}}{60\Phi(1 - 10^{-A_e})\left(\frac{A_{PS}}{A_e}\right)} \quad \text{Equation S2}$$

where η_{CAT} (μmol) is the number of mol of catalyst used in the photocatalytic system, Φ ($\mu\text{mol s}^{-1}$) is the photon flux determined by standard ferrioxilate actinometry, A_e is the total absorption of the sample at the irradiation wavelength (here 450 nm), A_{PS} is the absorbance at 450 nm due to the PS only, TOF_{max} is the maximum turnover frequency which is calculated according to the literature.¹⁰

Protein expression and purification

The plasmid for the expression of CB5 was kindly provided by the laboratory of Prof. Marcellus Ubbink. CB5 was expressed in *Escherichia coli* BL21 PLYS and purified as detailed in Opdam *et al* 2022.¹¹

Site-directed mutagenesis was performed to introduce the H20Y, H31Y and H85Y mutations *via* the WholePlasmid Synthesis (WOPS) protocol,¹² using the primers found in the table below. The primers were obtained from Sigma-Aldrich (Missouri, USA), and the Pfu polymerase was produced in-house. The correct incorporation of the mutations was checked using Sanger sequencing data (Baseclear BV, Leiden, The Netherlands).

Mutation	5' Mod	Sequence	3' Mod
H20Y	CCC TGG AAG AAA TTC AAA AAT ACA ATA ACT CTA AAT CTA CCT GGC	T L E E I Q K Y N N S K S T	GCC AGG TAG ATT TAG AGT TAT TGT ATT TTT GAA TTT CTT CCA GGG
H31Y	CCT GGC TGA TCC TGT ATT ATA AAG TGT ACG ATC TGA CC	T W L I L Y Y K V Y D L T	GGT CAG ATC GTA CAC TTT ATA ATA CAG GAT CAG CCA GG
H85Y	GCA AAA CCT TTA TCA TTG GCG AAC TGT ACC CGG ACG ACC GTT AAC TCG	S K T F I I G E L Y P D D R - L	CGA GTT AAC GGT CGT CCG GGT ACA GTT CGC CAA TGA TAA AGG TTT TGC

Teale's method to prepare apoCB5

Haem was removed from cytochrome B5 using Teale's method.¹³ The pH of the protein sample was lowered to 2.0 by dropwise addition of 0.5 M HCl under constant stirring on ice. An equal volume of ice-cold 2-butanone was added and mixed, then pipetted off after the layers had separated, and this procedure was repeated 2-3 times until a colourless aqueous solution was obtained. The aqueous layer was pipetted directly into a 3.5 kDa cut-off dialysis bag (cellulose dialysis tubing from Spectrum Chemical, California, USA) and dialyzed against 2 L of 20 mM sodium phosphate buffer solution at pH 7.5 at 4 °C overnight. The dialysis buffer was exchanged once after 120 min of dialysis. To improve sample stability traces of 2-butanone were removed using 2 stacked 5 mL HiTrap desalting columns from Sigma Aldrich (Missouri, USA) to exchange to 20 mM NaPi pH 8.0. UV-Vis was used to verify that the protein was in the *apo* state. *ApoCB5* was re-concentrated and stored frozen (with liquid N₂) at -80 °C until use.

Protein-catalyst complex preparation

For the preparation of ArM1 and ArM2, *apoCB5* from concentrated stock was reacted with CoSalen from a 4 mM stock in DMF (note that for NMR a 1 mM stock in milliQ was used) in respectively a 1:1 and 1:5 molar ratio, the final protein concentration during the reaction was 20 μM (so that the CoSalen concentrations were 20 μM or 100 μM, respectively). For the preparation of ArM3, *holoCB5* was reacted with CoSalen in a 1:5 molar ratio under the same conditions. The reactions were performed at 4 °C, overnight, on a Stuart STR9 roller from Sigma Aldrich (Missouri, USA) at 33 rpm. The resulting sample was concentrated to < 2 mL using a 20 mL, 5.000 kDa cut-off concentrator (Corning, New York, USA). DMF and excess CoSalen were removed using 2 stacked 5 mL HiTrap desalting columns from Sigma Aldrich (Missouri, USA) to exchange to 80 mM NaPi pH 7.5. The concentration of protein was determined using a BCA protein assay kit from Bio-Rad (California, USA). The CoSalen concentrations were determined using ICP-MS as detailed above. The samples were finally re-concentrated and stored frozen (with liquid N₂) at -80 °C until use.

For HR-MS measurements, samples containing only the protein were placed in a UV-Vis cuvette and irradiated during a period of 160 min (see Figure S1 for setup). A high-resolution spectrogram of each sample was measured following irradiation.

Water oxidation measurements

For every dataset, the black line represents the average of the 2 measurements. The coloured traces represent the SD of all the measurements done for each set of data. All photocatalysis was carried on in degassed phosphate buffer pH 7.5, 80 mM, containing 50 μM of the catalyst (CoSalen or CoSalen-protein adduct), 0.3 mM of [Ru(bpy)₃](ClO₄)₂ and 5 mM of Na₂S₂O₈. The 450 nm LED-based light source was set at an intensity of 350 mA, which provided an optical power of 18-19 mW measured with an OPHIR (Jerusalem, Israel) Nova-Display laser power meter as mentioned. Data processing was performed according to the literature.¹⁰ The average curve of each set of data was plotted using Origin 9.1 using the following method: Select set of values → Statistics → descriptive statistics → statistics on Row → Compute Mean. Using the same software, the error was plotted using 5% of SD and then corrected with the next script: Statistics → descriptiv statistics → statistics on Row → Compute SD. All the O₂ evolution data were fitted using Origin 9.1 using the following method: Analysis → Fitting → Non-linear curve → Growth/Sigmoidal category → Hill1 function. The Hill1 function is described by equation S3:

$$y = START + (END - START) \frac{x^n}{(k^n + x^n)} \quad \text{Equation S3}$$

pH titration *apoCB5*

For the determination of the pKa of the histidines in *apoCB5* an NMR titration was used in the range of pH 6.0-8.0. The chemical shift vs. the pH was fitted in Igor Pro version 6.37 from WaveMetrics (Oregon, USA) using the following equation:

$$\delta_{obs} = \frac{\delta L + \delta HL * 10^{pH - pKa}}{1 + 10^{pH - pKa}}$$

Equation S4

In which δ_{obs} is the observed chemical shift, δL is the chemical shift obtained in the lower pH limit, and δHL is the chemical shift obtained in the upper pH limit. The error in the chemical shift was based on the full width at half of the peak maximum and a 1.0% error was used for the solvent pH.

Supplementary C: Supplementary tables

Table S1. Stability of ArM2 monitored by the protein:cobalt ratio determined after repeated purification over P6 spin columns

ArM2	Ratio [Co] / [<i>apoCB5</i>] (sDev)
Purified 1x*	3.71 (0.14)
Purified 2x	3.69 (0.21)
Purified 3x	3.97 (0.15)

*Was purified by desalting column

Table S2. Assignment of histidine side chain proton chemical shifts (see Figure 6C for ring labelling) from LSW HSQC NMR spectra of *apoCB5* (top), ArM1 (middle) and ArM2 (bottom).

Sample	Assignment	Chemical shift ¹⁵ N (ppm)
<i>ApoCB5</i>	H85 Nε2	164.67
	H31 Nε2	178.23
	H44/68 Nε2	177.98
	H44/68 Nε2	180.43
	H44/68 Nδ1	212.79
ArM1	H85 Nε2	164.67
	H31 Nε2	177.49
	H44/68 Nε2	178.35
	H44/68 Nε2	161.50
	H44/68 Nε2	180.55
ArM2	H85 Nε2	164.67
	H31 Nε2	161.62
	H31 Nδ1	174.32
	H44/68 Nε2	162.59
	H44/68 Nδ1	173.95
	H44/68 Nε2	166.38
	H44/68 Nδ1	~174

Table S3. Assignment of histidine side chain nitrogen chemical shifts (see Figure 6C for ring labelling) from LSW HSQC NMR spectra of *apoCB5* (top), ArM1 (middle) and ArM2 (bottom).

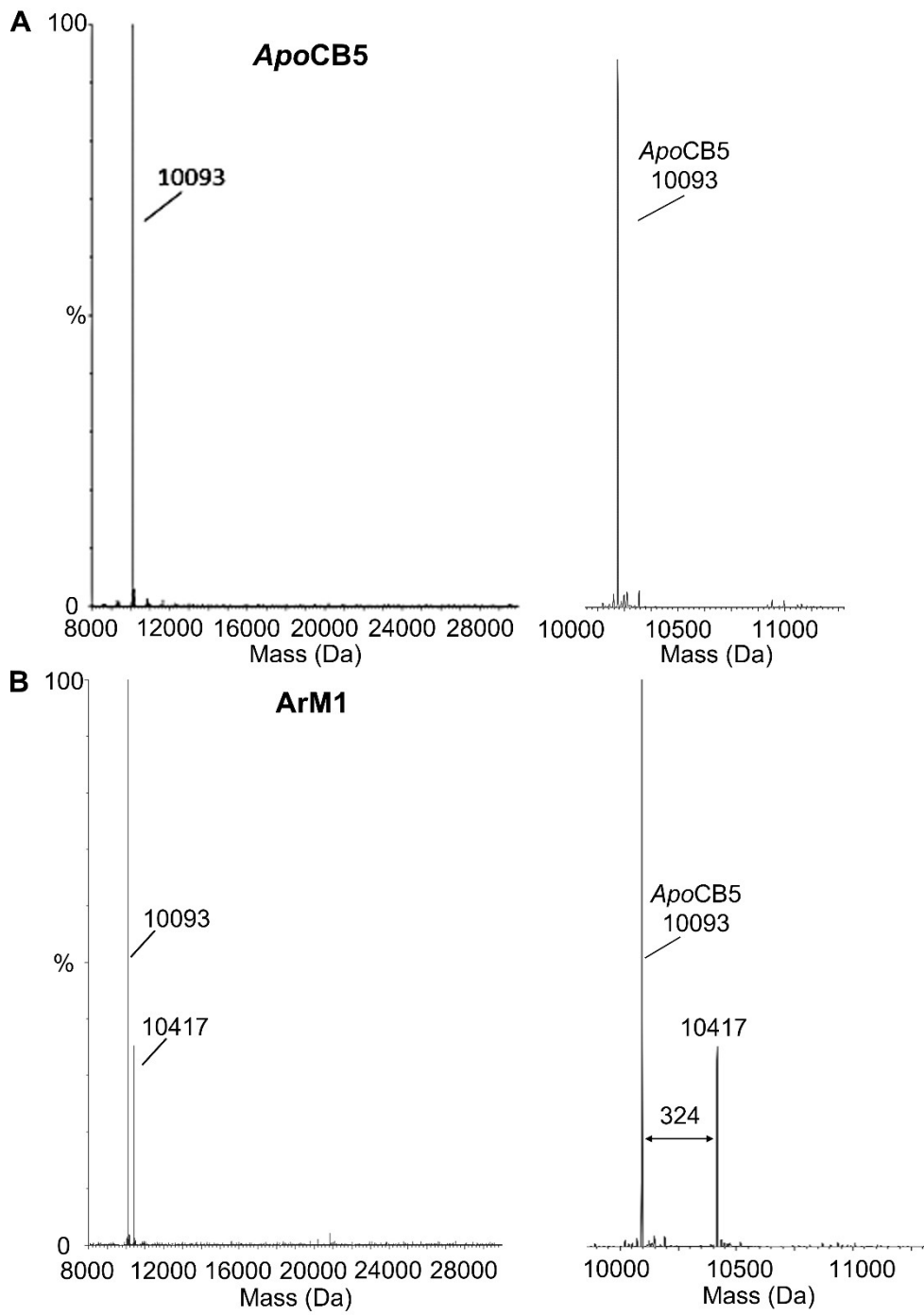
Sample	Assignment	Chemical shift ¹ H (ppm)
<i>ApoCB5</i>	H85 Hδ2	6.86
	H85 Hε1	7.39
	H31 Hδ2	6.72
	H31 Hε1	7.67
	H44/68 Hδ2	6.93
	H44/68 Hε1	7.76
	H44/68 Hδ2	6.89
	H44/68 Hε1	7.78
	H85 Hδ2	6.86
	H85 Hε1	7.39
ArM1	H31 Hδ2	6.74
	H44/68 Hδ2	6.93
	H44/68 Hδ2	6.24
	H44/68 Hδ2	6.89
	H44/68 Hδ2	6.19
	H85 Hδ2	6.86
ArM2	H85 Hε1	7.39
	H31 Hδ2	6.39
	H44/68 Hδ2	6.25
	H44/68 Hδ2	6.19
	H44/68 Hδ2	6.19

Table S4. Ratios of absorbances (A) at 280 nm and 450 nm for each of the fractions of ArM2 purified by SEC-MALS.

Multimer	Monomer	Dimer	Trimer	Tetramer	Larger oligomers
Ratio →	A_{280} / A_{450}				
Sample ↓					
Expected	10.5	10.5	10.5	10.5	10.5
Before	12.1	11.6	11.3	11.2	12.0
Dark	11.5	10.5	10.5	10.5	10.8
0.5 min	9.5	9.4	9.4		9.4
120 min	6.0	5.9	5.8		5.7

Conditions: The before sample contains only ArM2, the dark sample contains ArM2, $[\text{Ru}(\text{bpy})_3](\text{ClO}_4)_2$ and $\text{Na}_2\text{S}_2\text{O}_8$, the irradiated samples contain ArM2, $[\text{Ru}(\text{bpy})_3](\text{ClO}_4)_2$ and $\text{Na}_2\text{S}_2\text{O}_8$ and were irradiated with a 450 nm LED for respectively 0.5 min and 120 min. The “expected” ratios were determined for a non-irradiated sample of ArM2 in absence of $[\text{Ru}(\text{bpy})_3](\text{ClO}_4)_2$ and $\text{Na}_2\text{S}_2\text{O}_8$.

Supplementary D: Supplementary figures



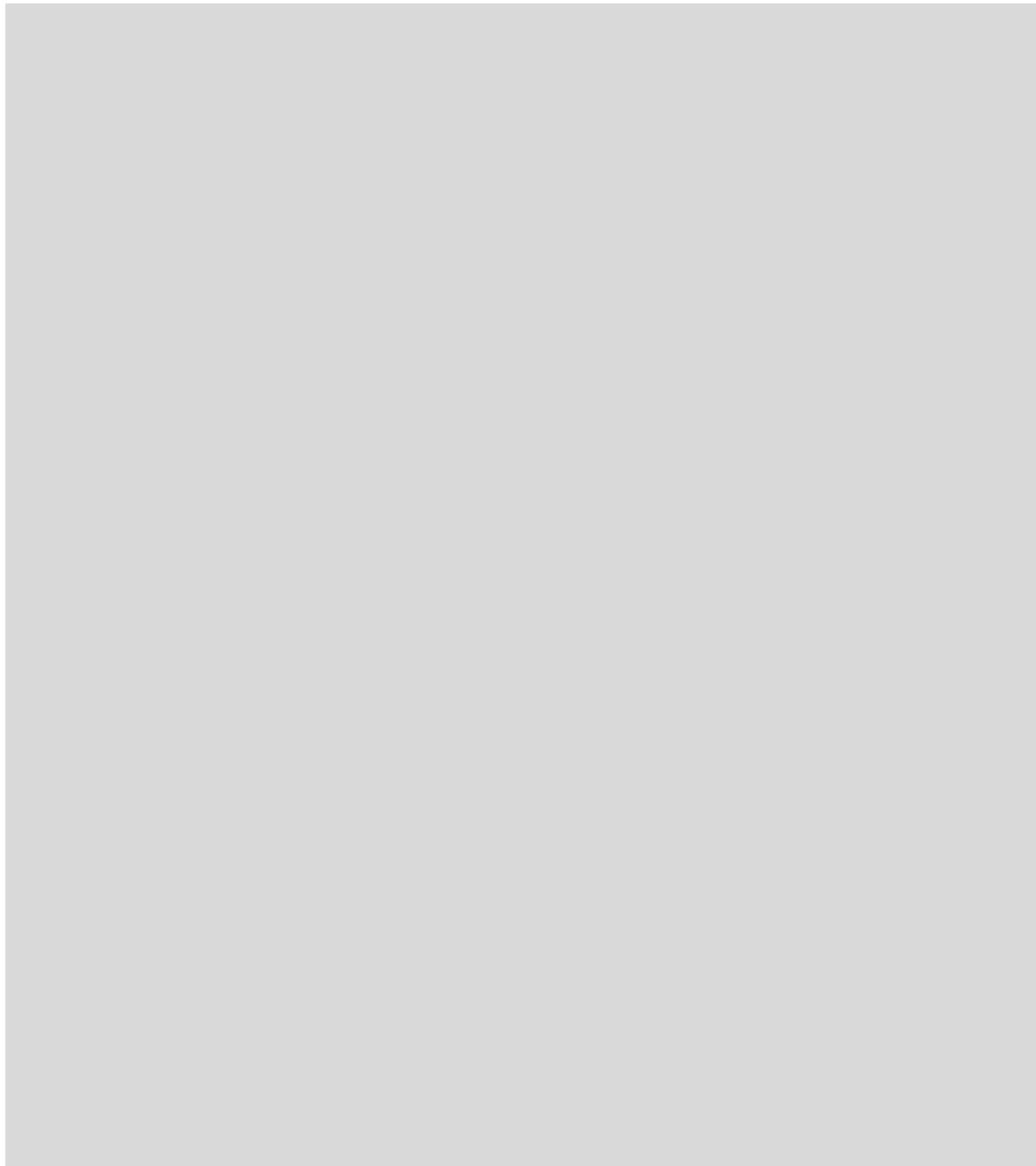


Fig. S3. Mass spectroscopy of the CB5 samples. In each case, a full spectrum is shown first, with on the left a zoom of any relevant regions. ApoCB5 (**A**), ArM1 (**B**), c. ArM3 (**C**), ArM2 (**D**).

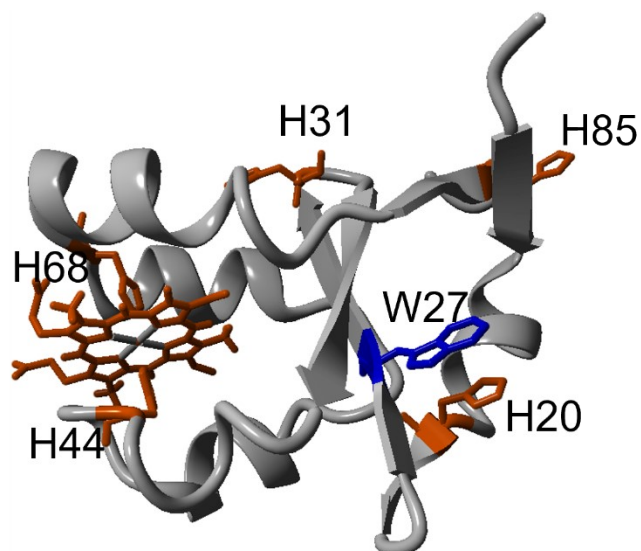


Fig. S4. Homology model of cytochrome B5 with all histidines (orange) and tryptophans (blue) shown explicitly (the homology model was prepared as detailed in supplementary A).

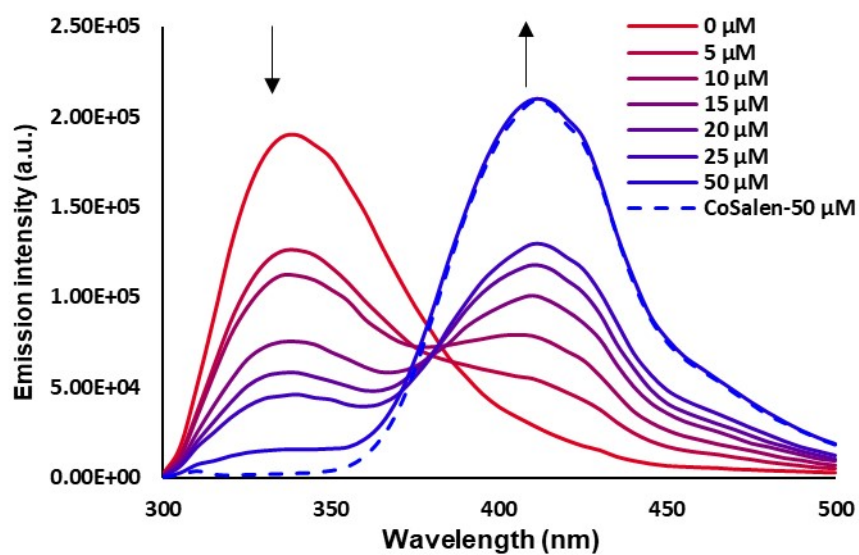


Fig. S5. Emission spectra of a titration of *apoCB5* with CoSalen in phosphate buffer pH 7.5. The excitation wavelength was 280 nm.

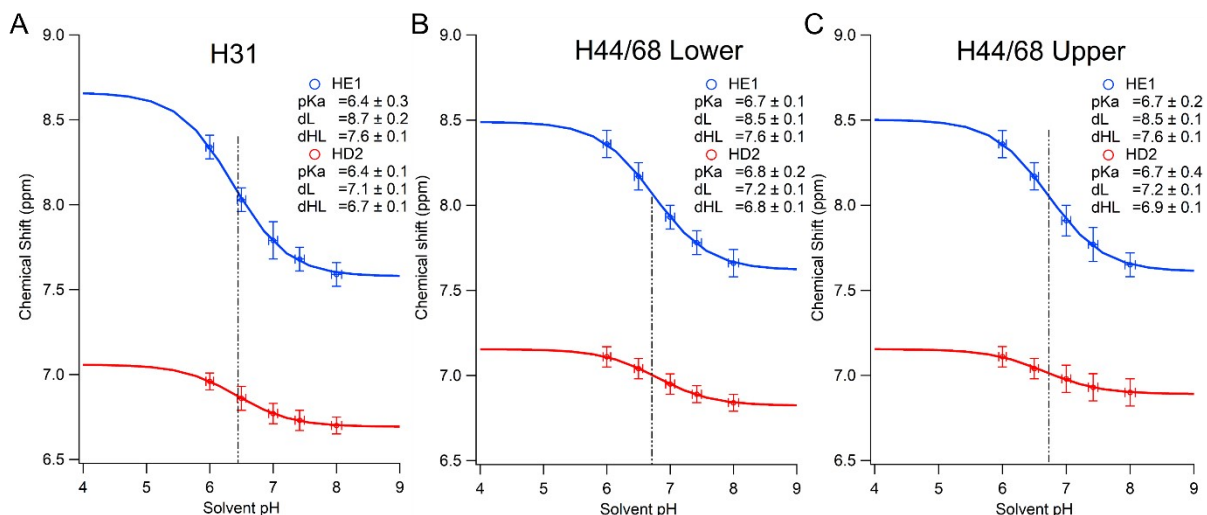


Fig. S6. The pH dependence per histidine side chain of *apoCB5* of the proton chemical shift as determined by large window HSQC NMR in the range pH 6.0-8.0. Data for H31 is shown in panel A, the more downfield (in the nitrogen dimension) of the two sets of peaks assigned to the binding pocket histidines (H44/H68) in panel B, the more upfield of the binding pocket histidines in panel C. The pK_a for each histidine is also indicated with a dotted line. In each panel the NE2 HE1 peak chemical shift and trace are given in blue and the NE2 HD2 peak chemical shift and trace in red. The data were fitted according to equation S4.

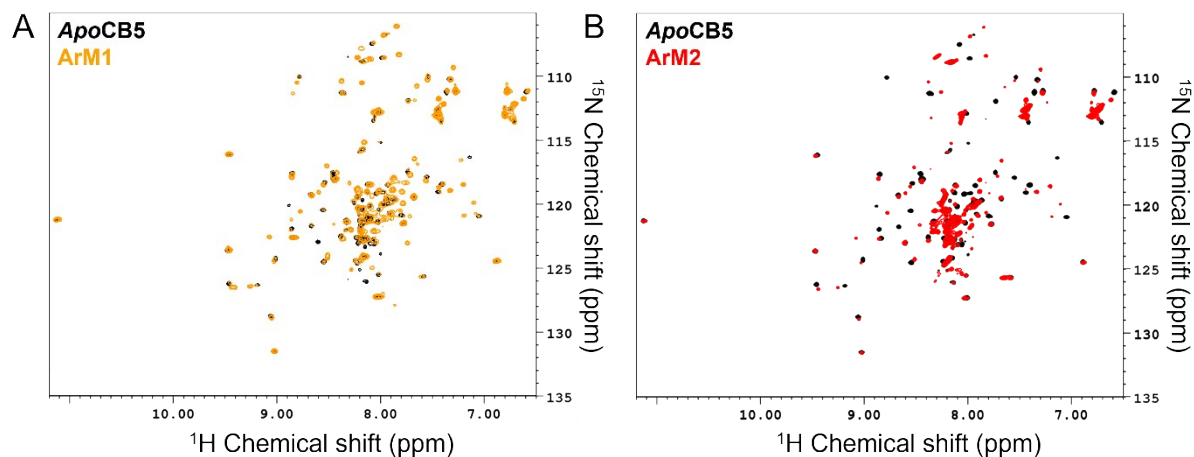
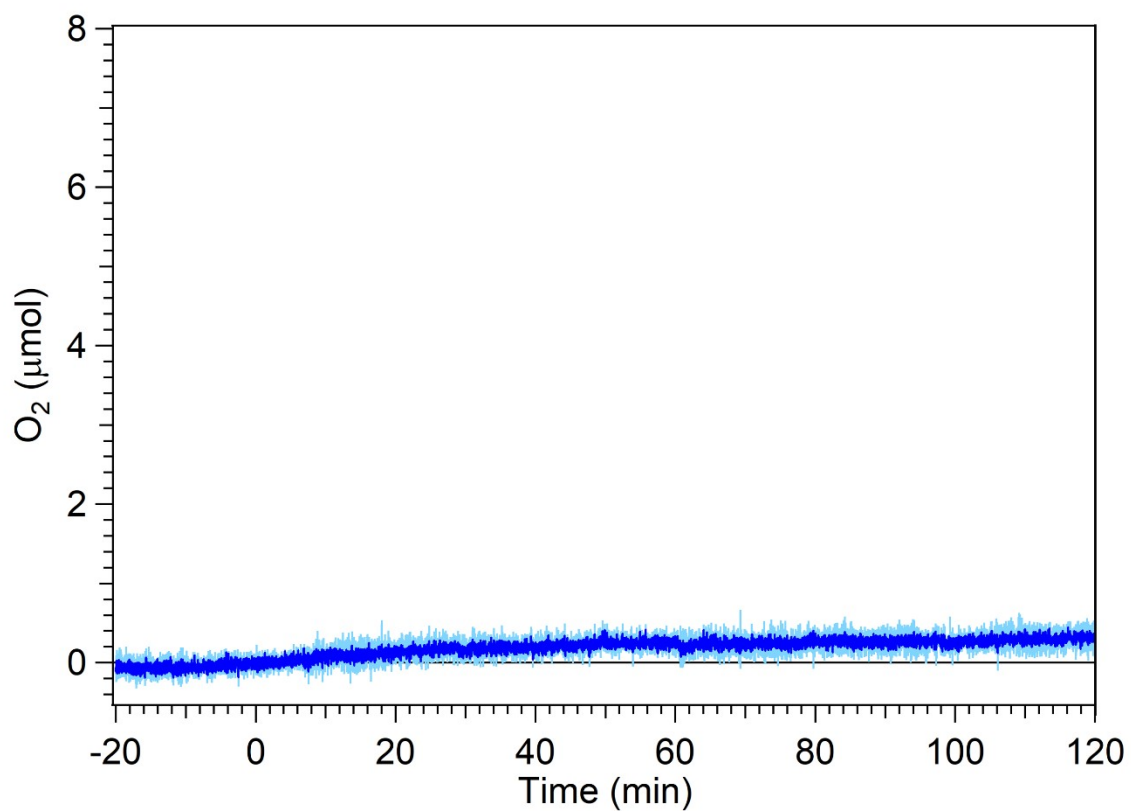


Fig. S7. HSQC NMR of *apoCB5* (black), ArM1 (A, orange) and ArM2 (B, red).



Fi

g. S8. Photoactivated water oxidation activity of 0.3 mM [Ru(bpy)₃](ClO₄)₂ and 5 mM Na₂S₂O₈ in 80 mM NaPi pH 7.5 upon irradiation with a 450 nm LED. The standard deviation is shown in light blue the average trace in dark blue. The trace is an average of 2 measurements.

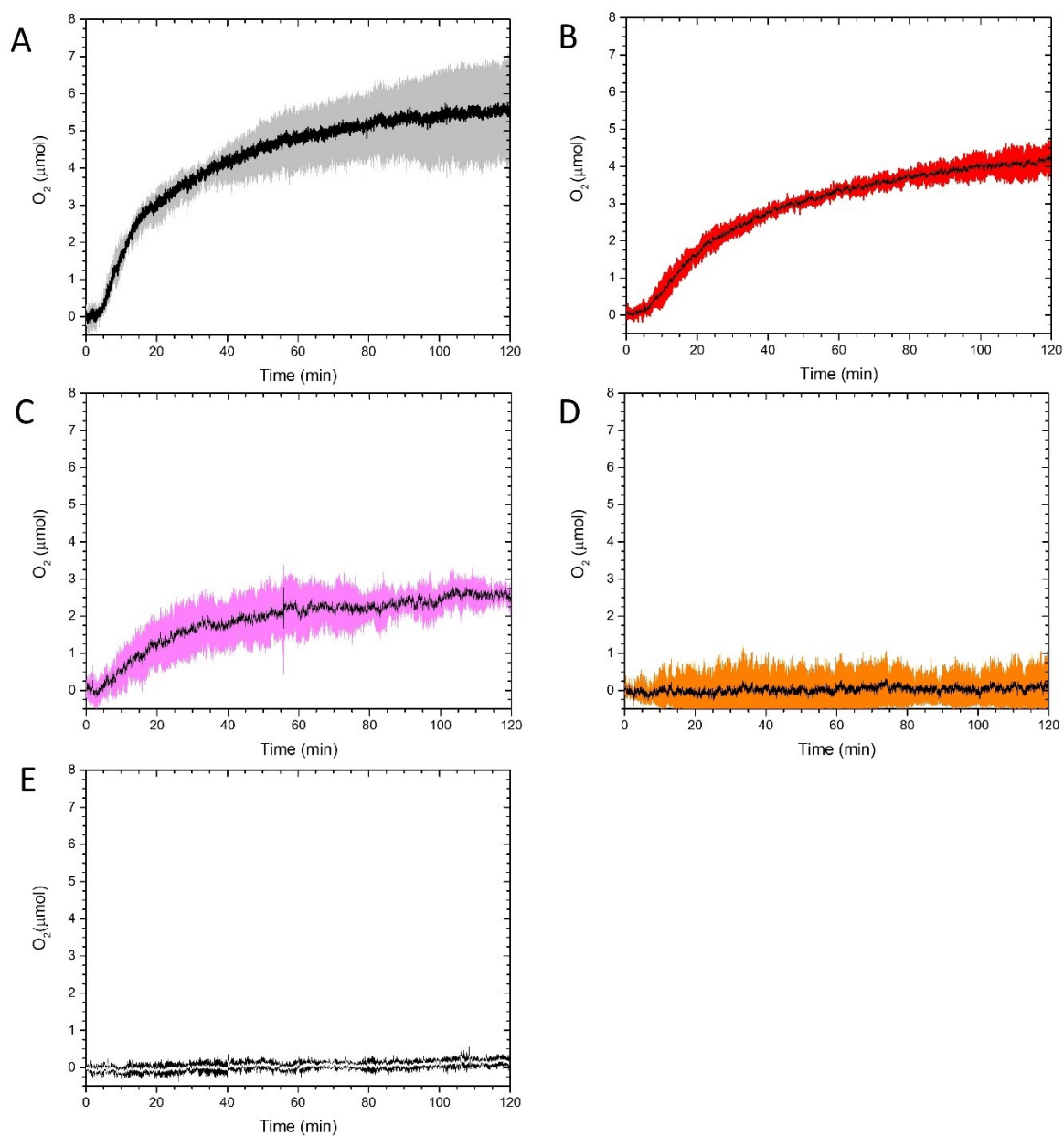


Fig. S9. Photoactivated water oxidation activity of CoSalen (A), ArM2 (B), ArM3 (C), ArM1 (D) and *apoCB5* (E) all with a CoSalen concentration of 50 μM (*apoCB5* in E was 50 μM in CB5), in the presence of 0.3 mM $[\text{Ru}(\text{bpy})_3](\text{ClO}_4)_2$ and 5 mM $\text{Na}_2\text{S}_2\text{O}_8$ upon irradiation with a 450 nm LED. The standard deviation is shown in colour surrounding the average trace in black (white in the case of *apoCB5*, E). Each trace is an average of at least 2 measurements.

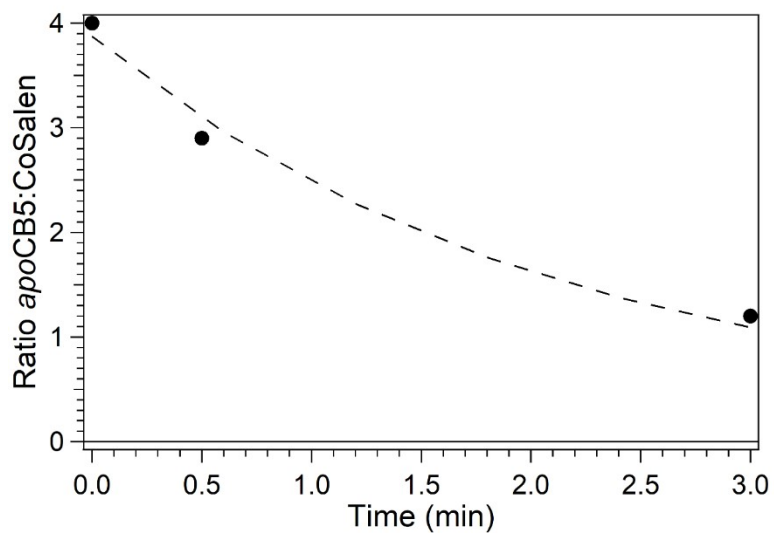


Fig. S10. The stability of ArM2 under photochemical conditions. The ratios of the amount of cobalt per CB5, determined by ICP-MS and a BCA kit after purification over a microspin Bio-Rad P6 column, are plotted for the ArM2 sample, and after 0.5 min and 3 min of irradiation at 450 nm in the photoreactor setup (see Figure S2) in the presence of $[\text{Ru}(\text{bpy})_3](\text{ClO}_4)_2$ and $\text{Na}_2\text{S}_2\text{O}_8$ (dots) with an exponential fit (interrupted line).

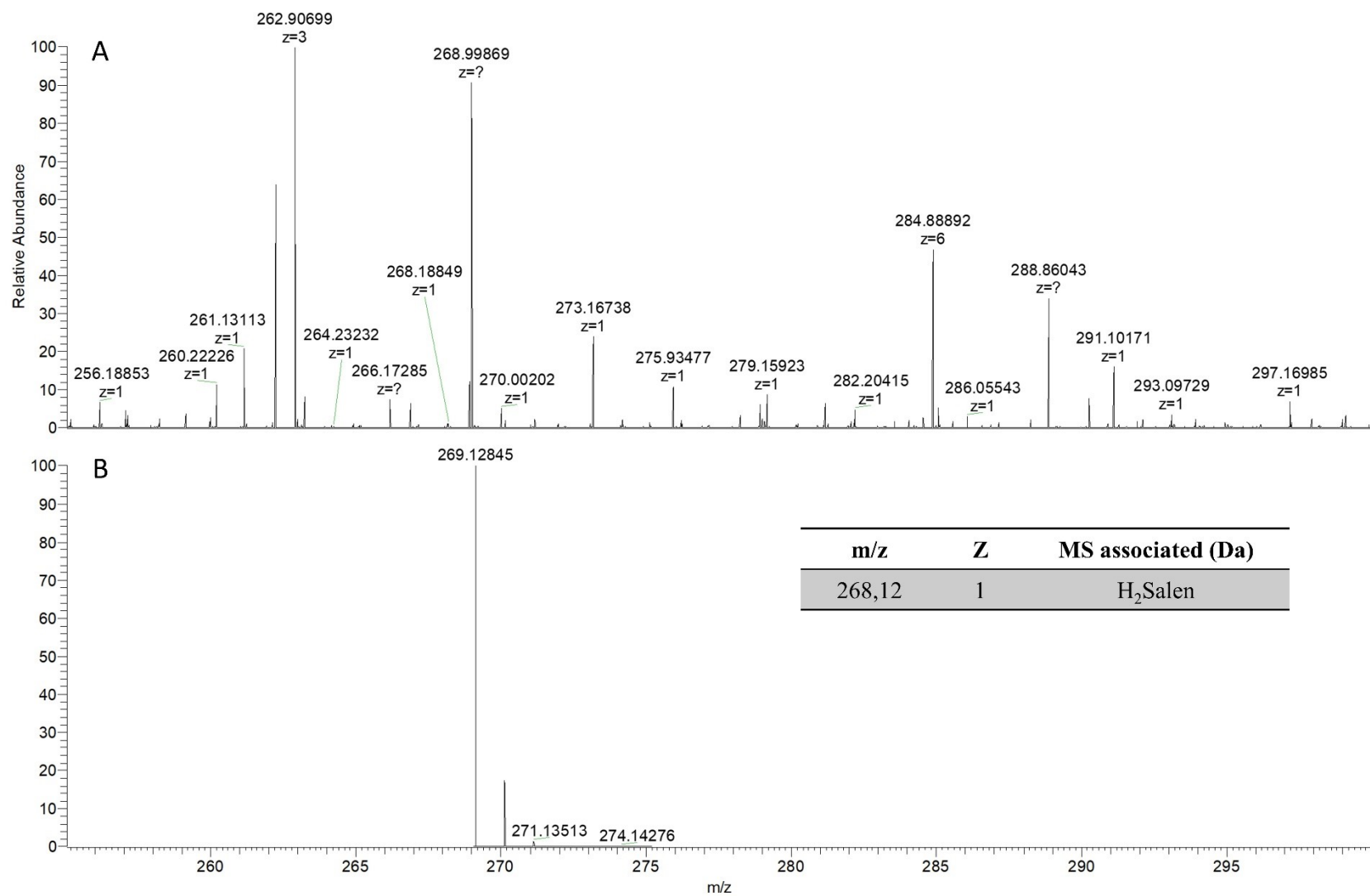


Fig. S11. Deconvoluted HR-MS of ArM2, [Ru(bpy)₃](ClO₄)₂ and Na₂S₂O₈ after photocatalysis, 120 min irradiation in phosphate buffer pH 7.5 80 mM. **(A)** Measured and **(B)** calculated for [M +H]

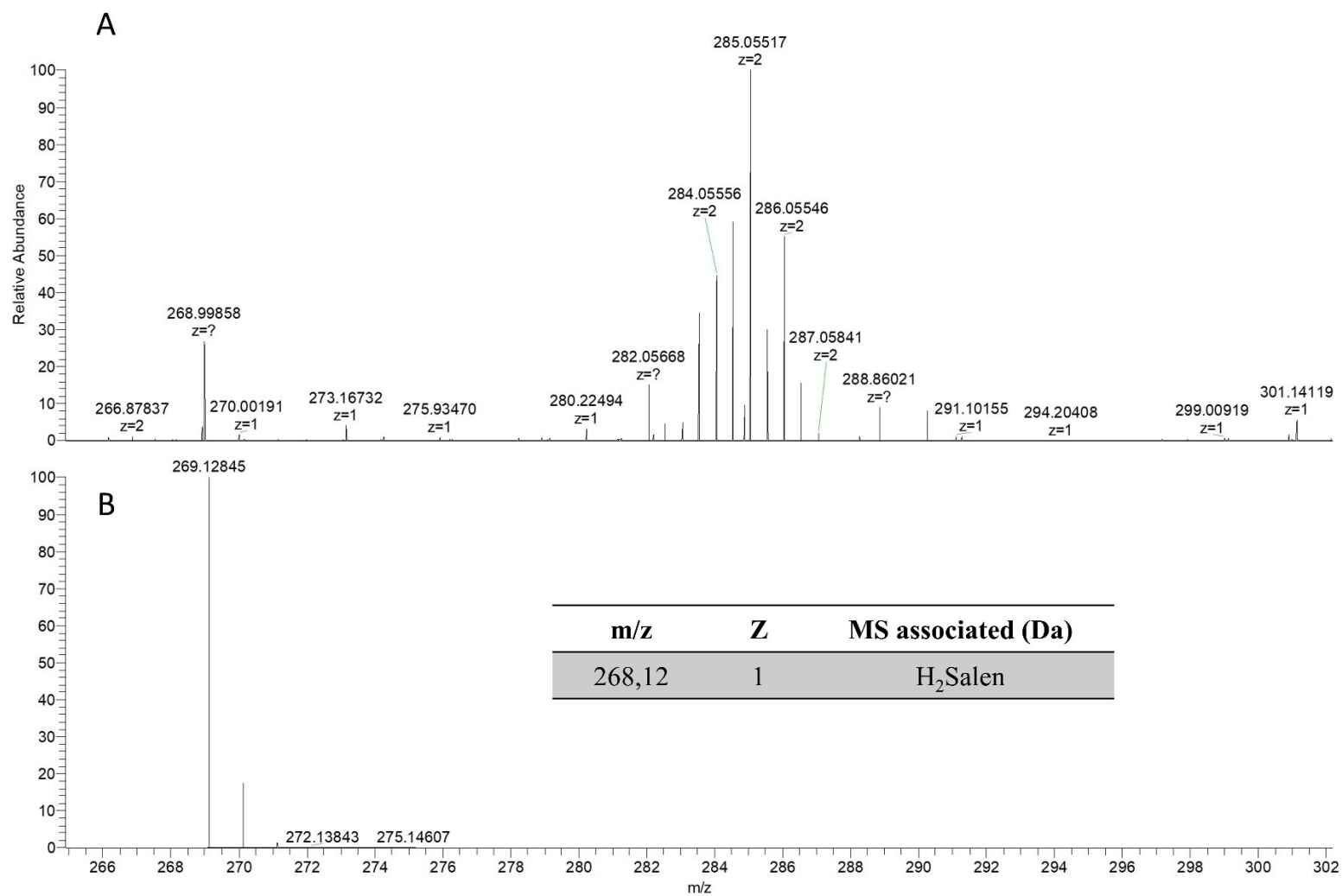


Fig. S12. Deconvoluted HR-MS of CoSalen, [Ru(bpy)₃](ClO₄)₂ and Na₂S₂O₈ after photocatalysis, 120 min irradiation in phosphate buffer pH 7.5 80 mM, 450 nm LED. (A) Measured and (B) calculated for [M +H]

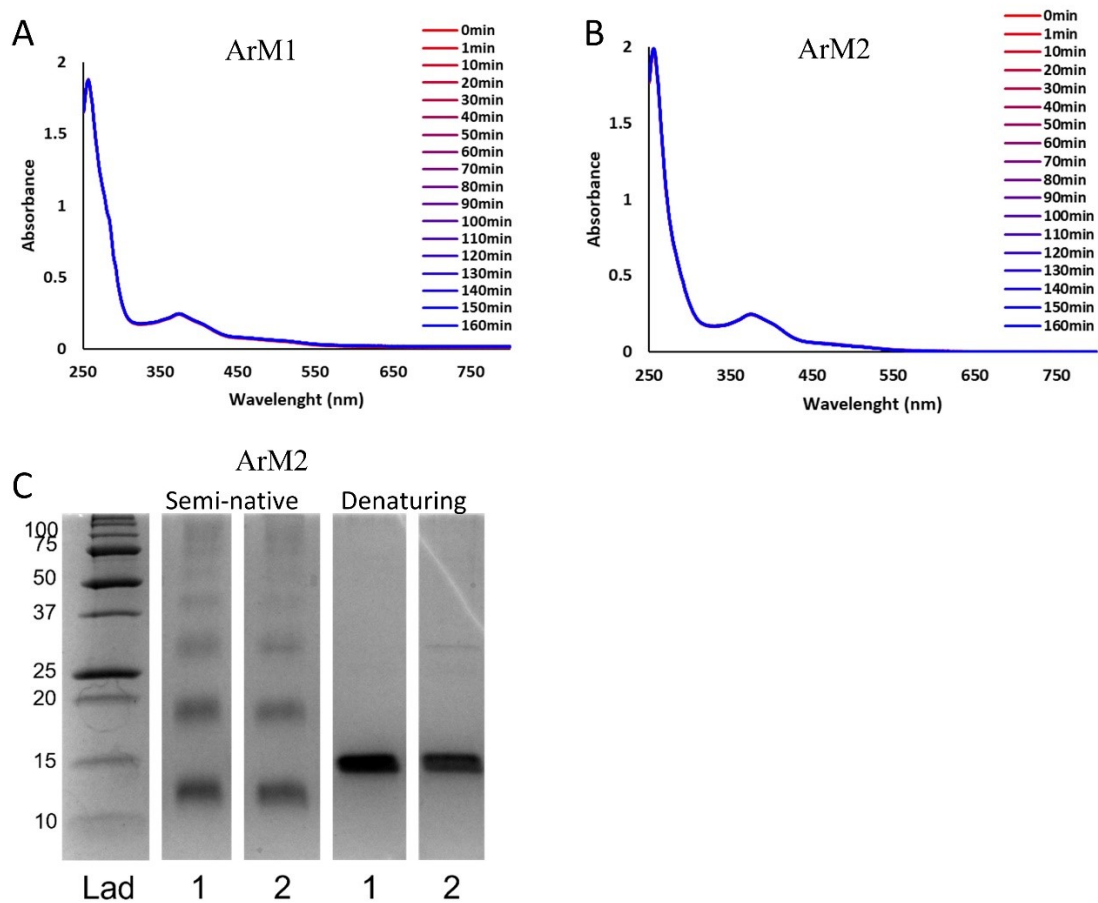


Fig. S13. UV-Vis-spectra of ArM1 (**A**) and ArM2 (**B**). Spectra were recorded vs. time for 160 min under constant irradiation using a 450 nm LED light source. All samples were measured in 80 mM NaPi buffer pH 7.5 with a protein concentration of 50 μ M. Red colour indicates $t=0$ min; blue colour indicates $t=160$ min., Semi-native (2nd and 3rd lane) and denaturing (4th and 5th lane) PAGE (**C**), visualized with coomassie, of ArM2 before irradiation (lanes 1) and after irradiation (lanes 2) with the protein ladder in the left-most lane with molecular weight in kDa indicated on the left.

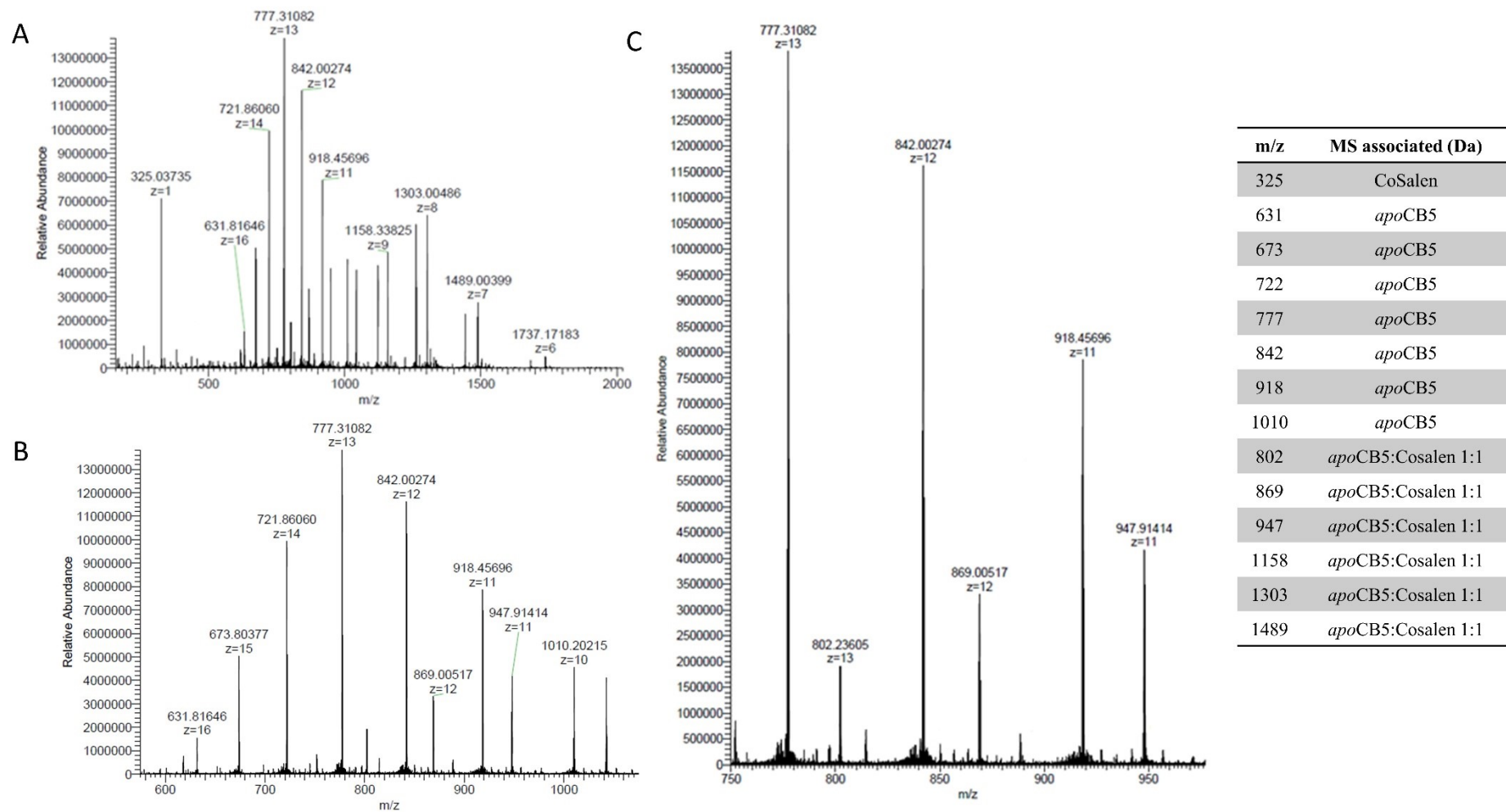
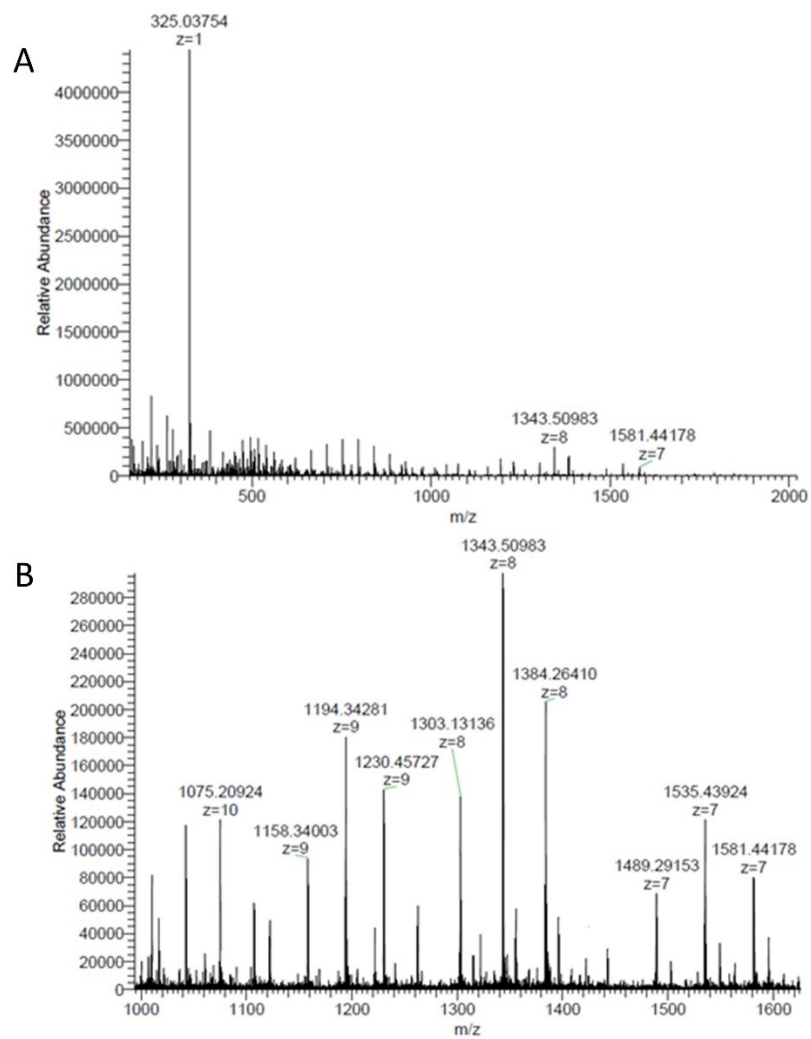


Fig. S14. Deconvoluted HR-MS of ArM1 after 160 min irradiation in phosphate buffer pH 7.5 80 mM, 450 nm LED. **(A)** from 0 to 2000 m/z; **(B)** from 600 to 1200 m/z; **(C)** from 750 to 980 m/z.



m/z	MS associated (Da)
325	CoSalen
1075	<i>apoCB5</i> :Cosalen 1:2
1158	<i>apoCB5</i> :Cosalen 1:1
1194	<i>apoCB5</i> :Cosalen 1:2
1230	<i>apoCB5</i> :Cosalen 1:3
1303	<i>apoCB5</i> :Cosalen 1:1
1343	<i>apoCB5</i> :Cosalen 1:2
1384	<i>apoCB5</i> :Cosalen 1:3
1489	<i>apoCB5</i> :Cosalen 1:1
1535	<i>apoCB5</i> :Cosalen 1:2
1581	<i>apoCB5</i> :Cosalen 1:3

Fig. S15. Deconvoluted HR-MS ArM2 after 160 min irradiation in phosphate buffer pH 7.5 80 mM, 450 nm LED. **(A)** from 0 to 2000 m/z; **(B)** from 1000 to 1600 m/z.

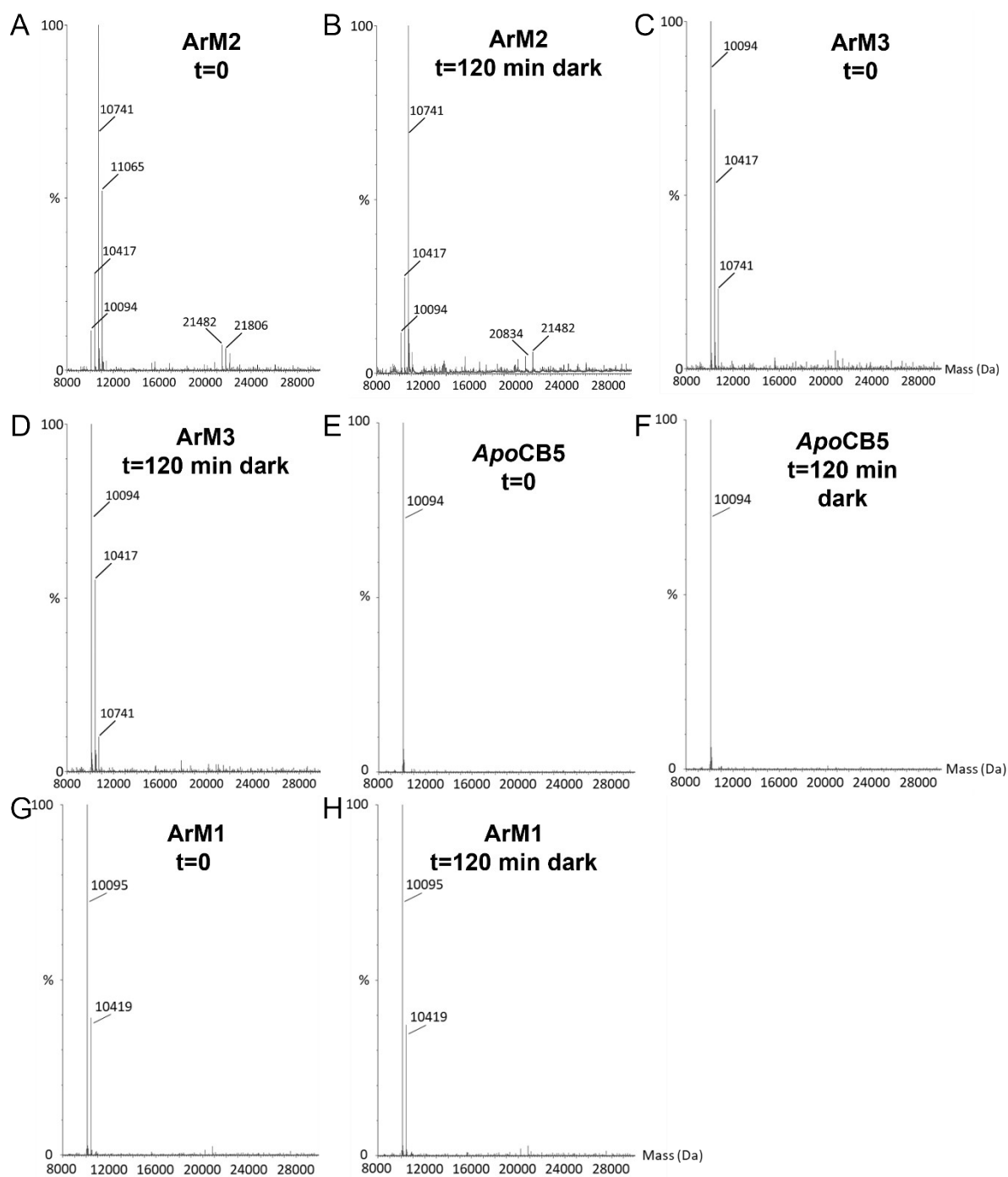


Fig. S16. Electron Spray Ionization Mass Spectrometry (ESI-MS) of the following samples, each in 80 mM NaPi pH 7.5 and kept dark and at room temperature after the addition of $[\text{Ru}(\text{bpy})_3](\text{ClO}_4)_2$ (0.3 mM) and $\text{Na}_2\text{S}_2\text{O}_8$ (5 mM), ArM2 t= 0 min (A), ArM2 t= 120 min (B), ArM3 t=0 min (C), ArM3 t= 120 min (D), apoCB5 t= 0 min (E), apoCB5 t= 120 min (F), ArM1 t= 0 min (G), ArM1 t= 120 min (H).

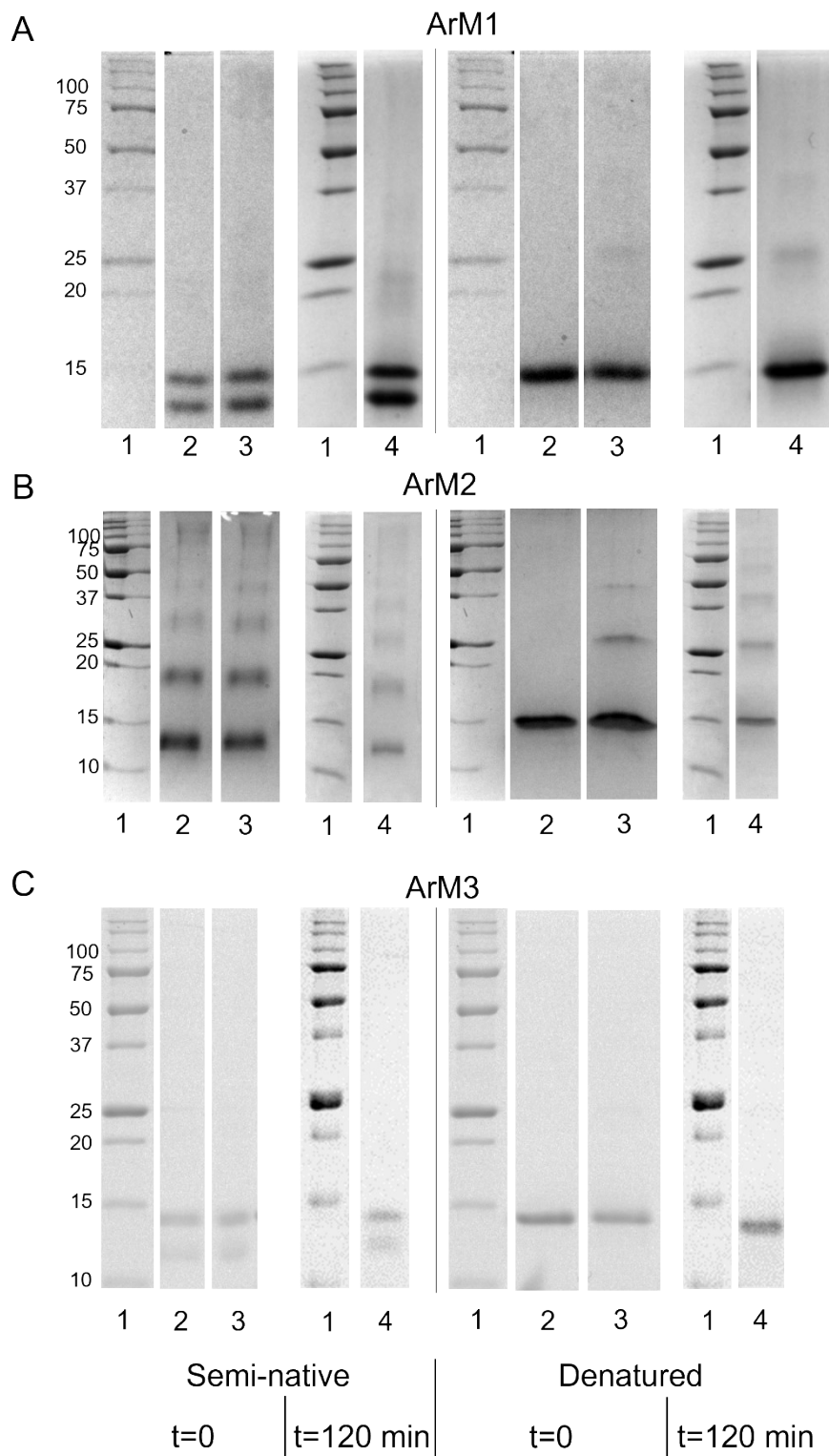


Fig. S17. Semi-native (left) and SDS (right) PAGE of ArM1 (A), ArM2 (B) and ArM3 (C), each in 80 mM NaPi pH 7.5 and kept dark and at room temperature (visualized with coomassie): Lanes 1: protein ladder with molecular weight indicated left, lanes 2: protein only, lanes 3: protein directly after the addition of $[\text{Ru}(\text{bpy})_3](\text{ClO}_4)_2$ (0.3 mM) and $\text{Na}_2\text{S}_2\text{O}_8$ (5 mM), lanes 4: protein + $[\text{Ru}(\text{bpy})_3](\text{ClO}_4)_2$ (0.3 mM) + $\text{Na}_2\text{S}_2\text{O}_8$ (5 mM) after 120 min.

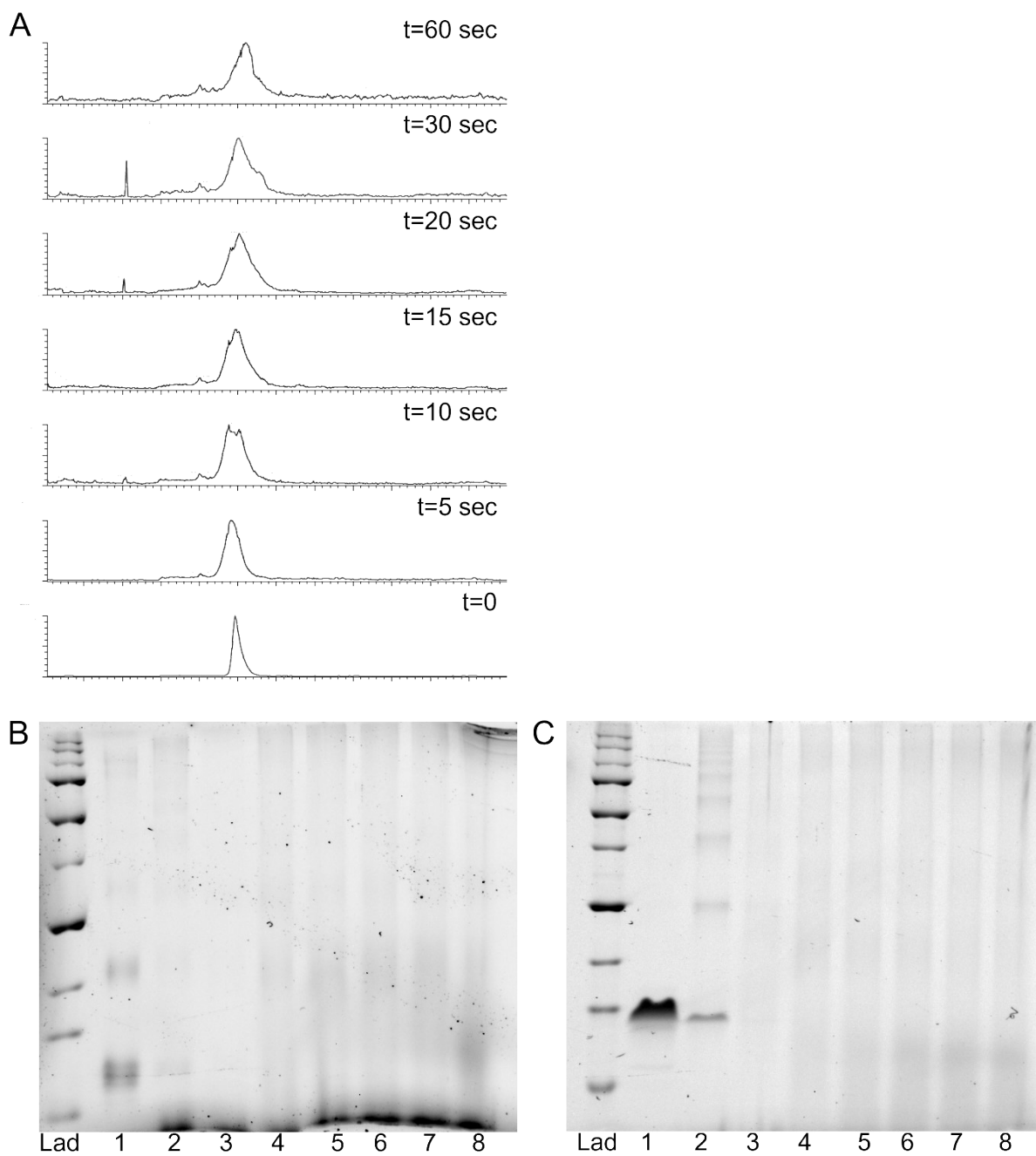


Fig. S18. Chromatograms of the C4 column run prior to mass spectrometry (A) of ArM2 + 0.3 mM $[\text{Ru}(\text{bpy})_3](\text{ClO}_4)_2$ + 5 mM $\text{Na}_2\text{S}_2\text{O}_8$ irradiated at 450 nm in the Clark setup for the time indicated in the figure. Semi-native (B) and denaturing (C) gel electrophoresis visualized with 2,2,2-trichloroethanol. Lane 1 contains ArM2, in lanes 2-8 0.3 mM $[\text{Ru}(\text{bpy})_3](\text{ClO}_4)_2$ and 5 mM $\text{Na}_2\text{S}_2\text{O}_8$ have been added and irradiation with a 450 nm LED in the Clark setup is performed for: Lane 2: 0 s, Lane 3: 5 s, Lane 4: 30 s, Lane 5: 60 s, Lane 6: 90 s, lane 7: 120 s and lane 8: 150 s

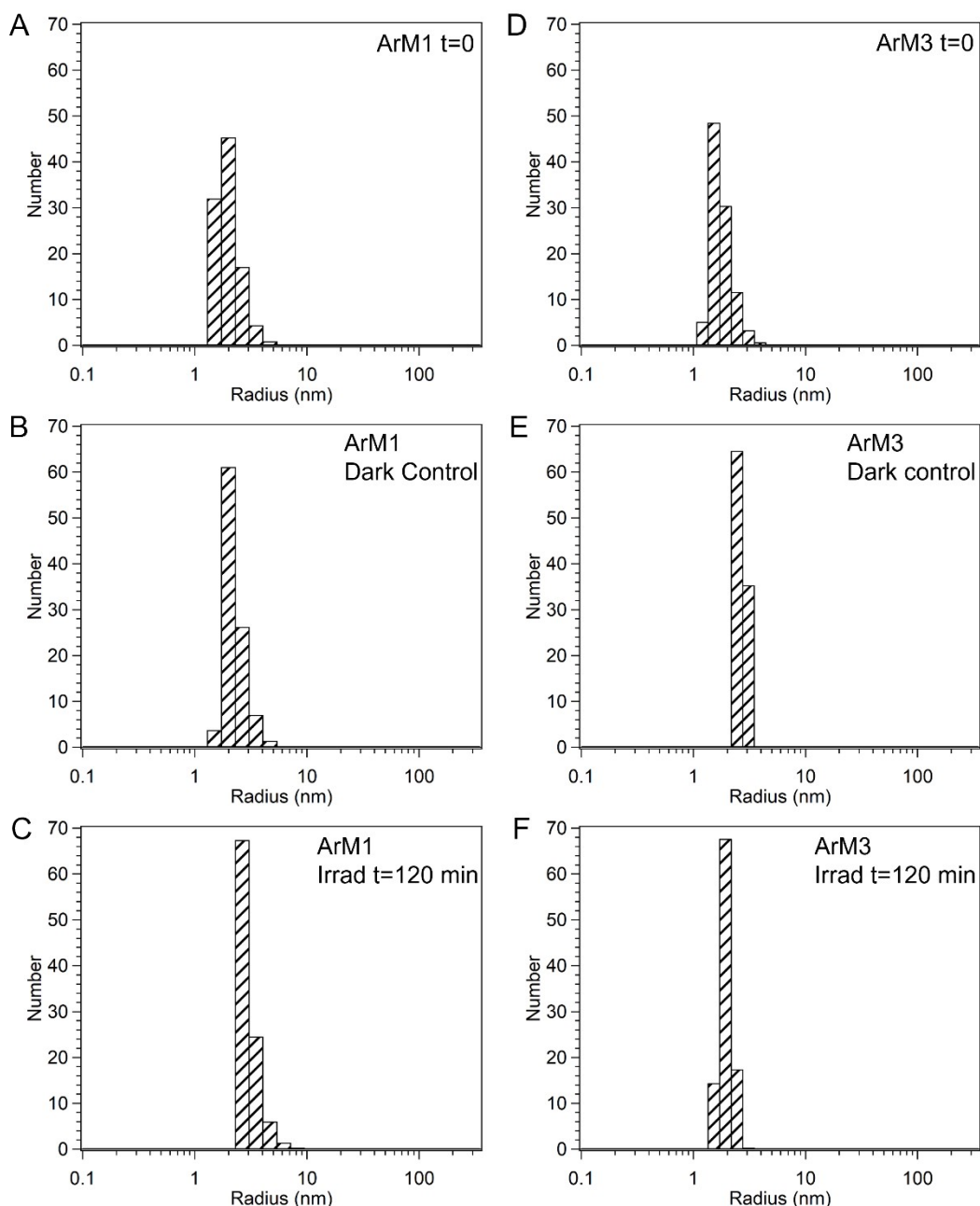


Fig. S19. Dynamic light scattering (DLS) analysis of ArM1 and ArM3 showing the percentage of the number of particles. All samples contain 50 μM CoSalen, either free or bound to CB5 in 80 mM NaPi pH 7.5. In the left panel the following graphs can be observed: DLS of ArM1 directly after the addition of 0.3 mM $[\text{Ru}(\text{bpy})_3](\text{ClO}_4)_2$ and 5 mM $\text{Na}_2\text{S}_2\text{O}_8$ (A), ArM1 + 0.3 mM $[\text{Ru}(\text{bpy})_3](\text{ClO}_4)_2$ + 5 mM $\text{Na}_2\text{S}_2\text{O}_8$ after 120 min dark at room temperature (B) and ArM1 + 0.3 mM $[\text{Ru}(\text{bpy})_3](\text{ClO}_4)_2$ + 5 mM $\text{Na}_2\text{S}_2\text{O}_8$ after 120 min irradiation at 450 nm at room temperature (C). On the right DLS of ArM3 directly after the addition of 0.3 mM $[\text{Ru}(\text{bpy})_3](\text{ClO}_4)_2$ and 5 mM $\text{Na}_2\text{S}_2\text{O}_8$ (D), ArM3 + 0.3 mM $[\text{Ru}(\text{bpy})_3](\text{ClO}_4)_2$ + 5 mM $\text{Na}_2\text{S}_2\text{O}_8$ after 120 min dark at room temperature (E) and ArM3 + 0.3 mM $[\text{Ru}(\text{bpy})_3](\text{ClO}_4)_2$ + 5 mM $\text{Na}_2\text{S}_2\text{O}_8$ after 120 min irradiation with a 450 nm LED at room temperature (F).

References

- (1) Fu, S.; Liu, Y.; Ding, Y.; Du, X.; Song, F.; Xiang, R.; Ma, B. *Chem Commun* 2014, **50**, 2167–2169.
- (2) Bienert, S.; Waterhouse, A.; De Beer, T. A.; Tauriello, G.; Studer, G.; Bordoli, L.; Schwede, T. *Nucleic Acids Res.* 2017, **45**, D313–D319.
- (3) Guex, N.; Peitsch, M. C.; Schwede, T. *Electrophoresis* 2009, **30**, S162–S173.
- (4) Waterhouse, A.; Bertoni, M.; Bienert, S.; Studer, G.; Tauriello, G.; Gumienny, R.; Heer, F. T.; de Beer, T. A. P.; Rempfer, C.; Bordoli, L. *Nucleic Acids Res.* 2018, **46**, W296–W303.
- (5) Studer, G.; Rempfer, C.; Waterhouse, A. M.; Gumienny, R.; Haas, J.; Schwede, T. *Bioinformatics* 2020, **36**, 1765–1771.
- (6) Bertoni, M.; Kiefer, F.; Biasini, M.; Bordoli, L.; Schwede, T. *Sci. Rep.* 2017, **7**, 1–15.
- (7) Falzone, C. J.; Mayer, M. R.; Whiteman, E. L.; Moore, C. D.; Lecomte, J. T. *Biochemistry* 1996, **35**.
- (8) Hirano, Y.; Kimura, S.; Tamada, T. *Acta Crystallogr. D Biol. Crystallogr.* 2015, **71**, 1572–1581.
- (9) Stoll, S.; Schweiger, A. *J. Magn. Reson.* 2006, **178**, 42–55.
- (10) Liu, C.; van den Bos, D.; den Hartog, B.; van der Meij, D.; Ramakrishnan, A.; Bonnet, S. *Angew. Chem. Int. Ed.* 2021, **60**, 13463–13469.
- (11) Opdam, L. V.; Polanco, E. A.; de Regt, B.; Lambertina, N.; Bakker, C.; Bonnet, S.; Pandit, A. *Anal. Biochem.* 2022, **653**, 114788.
- (12) Laible, M.; Boonrod, K. *J. Vis. Exp.* 2009, **27**, 1135.
- (13) Teale, F. W. J. *Biochim. Biophys. Acta* 1959, **35**, 543.